4.7 Waste Management

4.7.1 Yucca Mountain Heater Tests (15 p)

4.7.1.1 Heater Tests' Objective: Probing Thermally Driven Coupled Processes

Yucca Mountain, approximately 135 km northwest of Las Vegas, Nevada, has been designated as the site of the U. S. national geological repository for the permanent disposal of spent fuel and high-level radioactive waste. The geological formation in which the potential repository is situated is densely fractured welded tuff in the unsaturated zone a few hundred meters above the water table. The welded tuff has very small pores with strong capillarity effect, holding a significant amount of water in the matrix, and the matrix permeability of the welded tuff is low, on the order of microdarcies. However, this welded tuff is intensely fractured, with the permeability of these well-connected fractures many orders of magnitude larger than that of rock matrix. At thermodynamic equilibrium with the matrix at steady state, the fractures are essentially drained of water. Consequently, liquid and gas tend to flow in different parts of the rock formation: liquid predominantly in the low-permeability matrix and gas predominantly in the high-permeability fractures. At ambient conditions, the gas phase consists predominantly of air. However, in a nuclear waste repository, the heat generated from the decay of radioactive waste will cause water in the matrix pores to boil and greatly increase the vapor constituent in the gas phase. The pressure increase from vaporization drives the gas-phase transport by advection mainly through the fractures with its higher permeability and lower water saturation. Gas-phase diffusion driven by concentration gradient also occurs, because of the increase in water vapor (from boiling) and carbon dioxide (exsolved from the pore water with increasing temperature).

Heat from the anticipated decay of the radioactive waste would set in motion various coupled thermal, hydrological, mechanical and chemical processes. These thermally-driven coupled processes would affect the characteristics of the waste package environment, characteristics that control the corrosion of waste canisters and the mobilization rate of radionuclides. These coupled processes would also affect the rate of possible migration of radionuclides in the fractured rock away from the potential repository into the environment. To assess the impact of such heat-induced coupled processes on the safe performance of the repository, the United States Department of Energy (DOE) has been conducting *in situ* heater tests in an underground facility built into the unsaturated tuff at Yucca Mountain – the Exploratory Studies Facility (ESF). The primary objective of the ESF heater tests is to develop a better understanding of the coupled thermal, hydrological, mechanical, and chemical processes likely to exist in the Yucca Mountain rock mass surrounding the potential geological repository.

Gas-phase transport, the subject of this monograph, occurs in the heater tests as part of the coupled thermal-hydrological processes. We shall therefore, in the remainder of this chapter, focus our discussion on the observation of these thermal-hydrological processes, following a brief introduction of the general setting and configuration of the ESF heater tests, the Single Heater Test (SHT) and the Drift Scale Test (DST).

The ESF consists of an 8 km long tunnel with seven side alcoves for conducting underground experiments. The 8 m diameter tunnel descends gently through the different stratigraphic units of Yucca Mountain: from the alluvium at the surface, down through the Tiva Canyon welded and the Paintbrush nonwelded tuffs, and finally reaching the proposed repository horizon, the Topopah Spring welded tuff. As shown in Figure 1, both the SHT and the DST have been conducted in one of the side alcoves (Alcove 5) at the proposed repository horizon in the ESF.

The first heater test, the SHT, consists of a 5 m long rod heater, at a nominal rate of 4 kW, emplaced horizontally among 30 instrumental boreholes spanning a rock block of approximately 13 m by 10 m by 13 m. Figure 2 shows a schematic of the SHT borehole layout. The boreholes are numbered and color coded according to their functions: thermal, hydrological, mechanical, and chemical. The heater in the SHT was activated on August 26, 1996, for a heating phase of nine months (until the end of May 1997). Following a cooling phase of seven months, post-cooling field characterization activities began in January 1998. All testing activities and analyses have been completed for the SHT.

The second heater test, the DST, began its heating phase in December 1997 at a thermal rate of 187 kW for a heating period of four years. The heat in the DST was turned off on January 14, 2002, for a planned cooling phase of another four years. The DST is much larger than the earlier SHT. It has nine canister heaters placed in a 5 m diameter Heated Drift, running approximately east-west over a length of 47.5 m (Figures 1 and 3). Flanking the north and south sides of the Heated Drift are drilled fifty horizontal boreholes, twenty five drilled on each side of the Drift. Each of these boreholes houses an 11 m long rod heater, termed a wing heater. The Heated Drift and canister heaters have the same dimensions as the waste emplacement drift and the waste package, respectively, in the current repository design. The DST heating rate and the inclusion of the wing heaters were designed to heat a large volume of rock mass in a reasonably short testing period of a few years, so as to simulate the thermal-hydrological conditions reached after 50 to 100 years of waste emplacement in the repository. Close to 100 instrumented boreholes in the DST test block have been installed, with thousands of sensors monitoring thermal, mechanical, hydrological, and chemical conditions/parameters and data recorded on an

hourly basis. These boreholes are color-coded according to their functions in Figure. 3. Most boreholes labeled as “hydrological” and “chemical” do not originate from the Heated Drift; but rather from the Observation Drift that runs parallel to the Heated Drift at a distance of 30 meters from the Heated Drift axis. They are clusters of 40 m long boreholes forming vertical fans that bracket the Heated Drift and the wing heaters, primarily used for periodic active testing (geophysical logging and air-injection tests) to monitor time evolution and spatial distribution of drying and condensation zones in the test block. They are also used to collect water and gas samples for chemical and isotopic analysis.

4.7.1.2 Gas-Phase Transport in Heater Tests

Drying and wetting in different locations within the test block is the primary manifestation of the thermal-hydrological processes involving gas-phase transport (mainly vapor transport). As the formation temperature around the heater(s) approaches boiling (nominal boiling temperature is about 96^{o}C at the prevailing ambient pressure and elevation of the heater tests site), pore water in the rock matrix boils and vaporizes. Most of the vapor that is generated moves into the fractures, where it becomes highly mobile and is driven with the gas pressure gradient away from the heat source. When the vapor encounters cooler rock, it condenses. However, the increase in liquid saturation in the fractures from the condensate is likely to be small, since, because of the disparity of capillary suction forces in the fractures and matrix, a substantial amount of condensate will be imbibed into the matrix. In addition, because capillary suction is relatively weak in the fractures, we anticipate the condensate remaining in the fracture to drain downward by gravity. This drained condensate above the heater(s) would flow toward the heaters, boil again and then be transported away from the heaters to condense in the cooler rocks. The thermal-hydrological processes of continuous vaporization, gas transport, and

condensation leads to a decrease of rock-mass liquid saturation close to the heat source and an increase in rock-mass liquid saturation from condensate immediately outside of the drying zone. Over time, the drying zone expands during heating, with vapor transport the key process effecting the formation of drying and wetting zones in the fractured rock. The zones where all pore water have vaporized would correlate closely with temperature measurements above boiling. Prior to this, as long as water is still present while vaporization is taking place, two-phase conditions prevail and the temperature will remain at the nominal boiling point.

4.7.1.3 Measurements to Validate Vapor Transport Processes

Based on the discussion in the Section 4.7.1.2, observations of the gas-transport-driven thermal- hydrological processes in the heater tests are made in the following ways:

(1) Temperature is continuously monitored at various locations with respect to the heat source. Although vapor pressure continuously increases with rising temperature, thermal-hydrological processes do not become prominent until the temperature approaches boiling. Once a particular location within the test block reaches boiling, it is expected to remain at boiling for some time until all the mobile water surrounding the location of this particular temperature sensor is vaporized. Then the temperature will rise above boiling. It is safe to assume that the rock mass within the boiling isotherm (closer to the heat source) is “dry.” Hence, the passive monitoring temperature as a function of time at different locations within the rock mass provides indirect observation of the gas-transport processes.

(2) Geophysical methods sensitive to rock moisture content are applied in the heater tests. In both the SHT and DST, neutron logging, electrical resistance tomography, and cross-hole radar tomography have been carried out in different “hydrological” boreholes, at appropriate times throughout the tests, to track the spatial distribution and time evolution of the drying

and condensation zones. Since most water resides in the rock matrix in the welded tuff, changes in moisture content (detected by geophysical methods) reflect changes in the rock matrix.

(3) Air-injection tests are employed to probe slight changes in the very small fraction of water residing in the fractures. Air-injection tests are carried out periodically in borehole sections isolated by inflatable packers (in a subset of boreholes labeled "hydrological" in Figures 2 and 3). Any increase in liquid saturation from condensate results in increased resistance to air flow; hence, "wetting" of fractures is indicated by a decrease air permeability.

To illustrate vapor transport processes within fractures during the Yucca Mountain heater tests, we present below the air-permeability data collected over time from the SHT and DST.

4.7.1.3.1 Air-Permeability Measurements in the SHT

In the SHT, air-injection tests were carried out in boreholes 16 and 18 (see Figure 2) prior to heating, and also during heating and cooling phases, to track the changes in fracture liquid saturation. Note that boreholes 16 and 18 make up one of many pairs of boreholes labeled "hydrological" lying in a vertical plane orthogonal to the heater, intersecting the 5 m long heater at its midpoint. Two pairs of boreholes making the largest angle from horizontal (boreholes 24-25 and 26- 27) are used for conducting electrical resistance tomographic (ERT) measurements, while two other pairs of boreholes closer to the heater horizon are used for neutron logging and crosshole radar measurements. A pair of hydrological boreholes (holes 16 and 18) intended for air-injection tests make the smallest angle with respect to the heater horizon. Boreholes 16 and 18 were each installed with four high-temperature inflatable packers to separate the borehole into isolated sections, with an air-injection line and pressure sensor for each zone to facilitate air-permeability measurements. A typical test consisted of injecting air in one chosen zone at a

constant flow rate while monitoring pressure responses in this and all other isolated zones. The steady-state pressure response in the injection borehole itself can be used to estimate the local permeability, specific to the injection zone, averaged over the length of the packed-off zone. Assuming that air behaves as an ideal gas and that air flows through fractures are governed by Darcy's law, and that a finite line source can represent a borehole injection section, an analytical solution for ellipsoidal flow of incompressible fluid from a finite line source in an infinite medium is used to estimate permeability (Horvslev 1951; LeCain, 1995; Guzman et al., 1996):

$$k = \frac{P_{SC} Q_{SC} \mu \ln \frac{L}{r_w} T_f}{\pi L \left(P_2^2 - P_1^2\right) T_{SC}}. \qquad (4.7.1\text{-}1)$$

where

k	permeability (m^2)
L	length of air injection zones (m)
P_1, P_2	initial pressure and final steady state pressure for air injection tests (Pa)
P_{SC}	pressure at standard conditions, 1.013 x 10^5 Pa
Q_{sc}	flowrate at standard conditions in air injection tests (m^3/s)
r_w	radius of boreholes (m)
T_f	temperature of formation in air injection tests (^{o} K)
T_{SC}	temperature at standard conditions (273.15 ^{o}K)
μ	dynamic viscosity of air (Pa-s), 1.81 $\times 10^{-5}$ at 20 ^{o}C

Figure 4 shows the air-permeability measurements for zone 3 in boreholes 16 and 18. Zone 3 is the isolated borehole section between the bottom of the borehole and the fourth packer

farthest from the borehole collar. Zone 3 of borehole 16 spans a radial distance of 1.1 m to 3.2 m from the heater, and zone 3 of borehole 18 spans a radial distance of 1.5 m to 3 m from the heater. The horizontal axis of Figure 4 is the time line, with the heater activation and termination dates marked; the vertical axis is the measured air permeability. Graphs in Figure 4 show a decrease in air permeability (from the preheating values) by a factor of four and two, respectively, for zone 3 of boreholes 16 and 18, during the entire heating phase of the SHT. The air permeability returns to its preheating value[1] after the termination of heating.

Air-injection tests in the other zones in boreholes 16 and 18 closer to the borehole collar (or farther away from the heater) show no air-permeability decrease from their preheating values throughout the heating phase. These observations are consistent with the expected thermal-hydrological processes discussed in Section 4.7.1.2. This follows from the fact that temperature measurements in the SHT test block indicate that the boiling isotherm is at about 0.8 m radial distance from the heater after three months of heating, and moves out to about 1.2 m at the end of nine months of heating. Zone 3 of boreholes 16 and 18 are located within the condensate zone outside of the boiling isotherm, and thus they experienced a drop in air permeability during the heating phase. Other zones in boreholes 16 and 18 are too far removed from the boiling isotherm to experience any increase in liquid saturation that would result in a decrease of air permeability. During the cooling phase, air-permeability values return to their preheating values, since the cooling phase differs from the heating phase in that vaporization ceases while imbibition of condensate from the fractures into the rock matrix and gravity drainage continues. Without the continuous supply of vapor during the heating phase to replenish the accumulation of condensate

[1] In fact, the postheating values are slightly higher than the preheating values. Such postheating air-permeability increase is found generally in many other boreholes, which is hypothesized as indicative of the opening of fractures from thermal-hydrological-mechanically coupled processes (Tsang et al., 1999)

in the fractures that imbibe into the matrix or drain by gravity, little water enters the fractures, and the air- permeability values return to preheating values during the cooling phase.

4.7.1.3.2 Air-Permeability Measurements in the DST

Air-injection tests were carried out during the preheating and heating phases of the DST. Figure 5 shows the preheating baseline air-permeability measurements in the twelve (hydrological) boreholes that form three vertical fans. These three clusters are orthogonal to the Heated Drift, intersecting it at y =10 m (cluster of five boreholes labeled 57-61), y = 30 m (cluster of five boreholes labeled 74-78), and y = 40 m (pair of two boreholes labeled 185-186). Each 40 m long borehole was installed with high-temperature inflatable packers to isolate the borehole into four[2] 8 to 10 m sections. Each isolated zone (zone 1 being closest to the collar and zone 4 closest to the bottom of each borehole) was equipped with an air-injection line and pressure sensor. Air-permeability measurements were carried out in each of the 46 isolated zones in the 12 boreholes. The estimated perheating permeability for different zones of the hydrology holes ranged over three orders of magnitude, from 1.6×10^{-15} m^2 to 9.7×10^{-13} m^2.

During the heating phase of the DST, air-injection tests were repeated at approximately three-months intervals in the 12 boreholes. The air permeability in each zone was computed according to Equation 4.7.1-1, and normalized[3] to its respective pre-heating baseline value. These normalized values as a function of time with respect to heat activation are plotted in Figures 6, 7, and 8 for the three clusters of boreholes. A very clear trend of decrease in air permeability is seen in many of the 46 borehole sections. The time and magnitude of the decrease bears a clear correlation to the respective zone's proximity to the heat source. That is, as

[2] For two of the boreholes, boreholes 58 and 77, only three packers were installed because of numerous fractures and lithophysal cavities in the borehole walls.

heating continues, drying around the Heated Drift and the wing heaters expands, and the condensation front moves outward. The condensate causes a locally increased liquid saturation in the fractures and a corresponding decrease of permeability. It is largest in magnitude and occurs earliest in time in those zones closest to the wing heaters (e.g., zones 60-2, 60-3, 186-2, and 186-3). Those zones that are farthest from the heaters show no change or a slight increase in permeability from their preheating baseline values. No change in air permeability indicates that these zones are too far from the heated zone to experience an increase in liquid saturation from condensation. The slight increase in permeability may be attributed to the opening of fractures from thermal-mechanical coupled processes. Note also that with time, the drying zone expands, and those zones that at earlier times show a decrease of air permeability (because of condensate accumulation) become drying zones at later times, with permeability returning towards the preheating values. This is illustrated by the data for zones 60-3 and 59-3 in Figure 6. For zone 60-3, after a sharp drop in permeability at three months after heating, the permeability at nine months of heating returns to preheating baseline value. For 59-3, the permeability value decreases steadily until November 2000, after which the permeability increases, indicating drying.

4.7.1.3.3 Summary

We have carried out modeling of the thermal-hydrological processes of the SHT and DST, using the integral-finite-difference numerical simulator TOUGH2, developed by Pruess (1987, 1991), for simulating multidimensional transport of water, vapor, air, and heat in heterogeneous porous and fractured media. For both the SHT and DST, site-specific 3-D numerical models have been constructed, with the fractured welded tuff modeled as a dual continuum. The conceptual

[3] Missing data in Figures 6, 7, and 8 can be from two sources. One is when steady state pressure response is not attained, and the other is when packers separating certain zone became permanently damaged so that a comparison

model described in Section 4.7.1.2 is confirmed by these simulations, and the measured trends in air-permeability changes with time discussed in Sections 4.7.1.3.1 and 4.7.1.3.2 are consistent with simulated moisture redistribution of moisture performed by the 3D thermal-hydrological numerical model of the SHT (Tsang and Birkholzer, 1999) and the DST (Birkholzer and Tsang, 2000).

Acknowledgments

This work was supported by the Director, Office of Civilian Radioactive Waste Management, U. S. Department of Energy, through Memorandum Purchase Order EA9013MC5X between Bechtel SAIC Company, LLC and the Ernest Orlando Lawrence Berkeley National Laboratory (Berkeley Lab). The support is provided to Berkeley Lab through the U. S. Department of Energy Contract No. DE-AC03-76SF00098. The author thanks Chin-Fu Tsang and Dan Hawkes of Berkeley Lab, and…… for critical review of the manuscript and suggestions for improvement..

References

Birkholzer, J.T. and Tsang, Y.W., 2000. Modeling the thermal-hydrologic processes in a large-scale underground heater test in partially saturated fractured tuff, Water Resources Research, 36 (6), 1431-1447.

Guzman, A.G., A.M. Geddis, M.J. Henrich, C.F. Lohrstorfer, and S.P. Neuman, 1996. Summary of air permeability data from single-hole injection tests in unsaturated fractured tuffs at the Apache Leap Research Site; Results of steady-state interpretation, U.S. Nuclear Regulatory Commission Report NUREG/CR-6360, NRC, Washington DC.

Hvorslev, M.J., 1951. Time Lag and Soil Permeability in Ground-Water Observations. AEWES Bulletin 36. Vicksburg, Mississippi: U.S. Army Corps of Engineers, Waterways Experiment Station.

LeCain, G.D., 1995. Pneumatic testing in 45-degree-inclined boreholes in ash-flow tuff near Superior, Arizona, USGS Water Resources Investigations Report 95-4073, USGS, Denver, Colorado.

Pruess K., 1987. TOUGH user's guide, Technical Report LBL-20700, Lawrence Berkeley National Laboratory, Berkeley, California.

---

with baseline is no longer possible.

Pruess K., 1991. TOUGH2 –A general purpose numerical simulator for multiphase fluid and heat flow, Technical Report LBL-29400, UC-251, Lawrence Berkeley National Laboratory, Berkeley, California.

Tsang Y. W., Apps J., Birkholzer J. T., Peterson J., Sonnenthal E., Spycher N. and Williams K., 1999. Yucca Mountain Drift Scale Test progress report, Technical Report LBNL-42538, Lawrence Berkeley National Laboratory, Berkeley, California.

Tsang, Y.W. and Birkholzer, J.T., 1999. Predictions and Observations of the Thermal-hydrological conditions in the Single Heater Test. *J. of Contaminant Hydrology, 38(1-3)*, 385-425.

Figure Captions:

Figure 1. Schematic Plan View of ESF Thermal Test Facility Including the Single Heater Test (SHT) and the Drift Scale Test (DST)

Figure 2. Schematic SHT Layout of the Instrumental Boreholes, Color Coded According to Their Functions

Figure 3. Perspective View Showing Drifts and Boreholes of the DST, Boreholes Are Color Coded According to Their Functions

Figure 4. Air Permeability Measurements in Zone 3 of Boreholes 16 and 18 for before, during and after Heating Phase of the SHT

Figure 5. Preheating Baseline Permeability Measurements in Zones Isolated by Packers in Twelve 40 m Long Boreholes in the DST, the Permeability Values Range over Three Orders of Magnitude

Figure 6. Changes in Permeability Displayed as Ratio to the Preheating Permeability Estimate for DST Boreholes 57-61

Figure 7. Changes in Permeability Displayed as Ratio to the Preheating Permeability Estimate for DST Boreholes 74-78

Figure 8. Changes in Permeability Displayed as Ratio to the Preheating Permeability Estimate for DST Boreholes 185-186

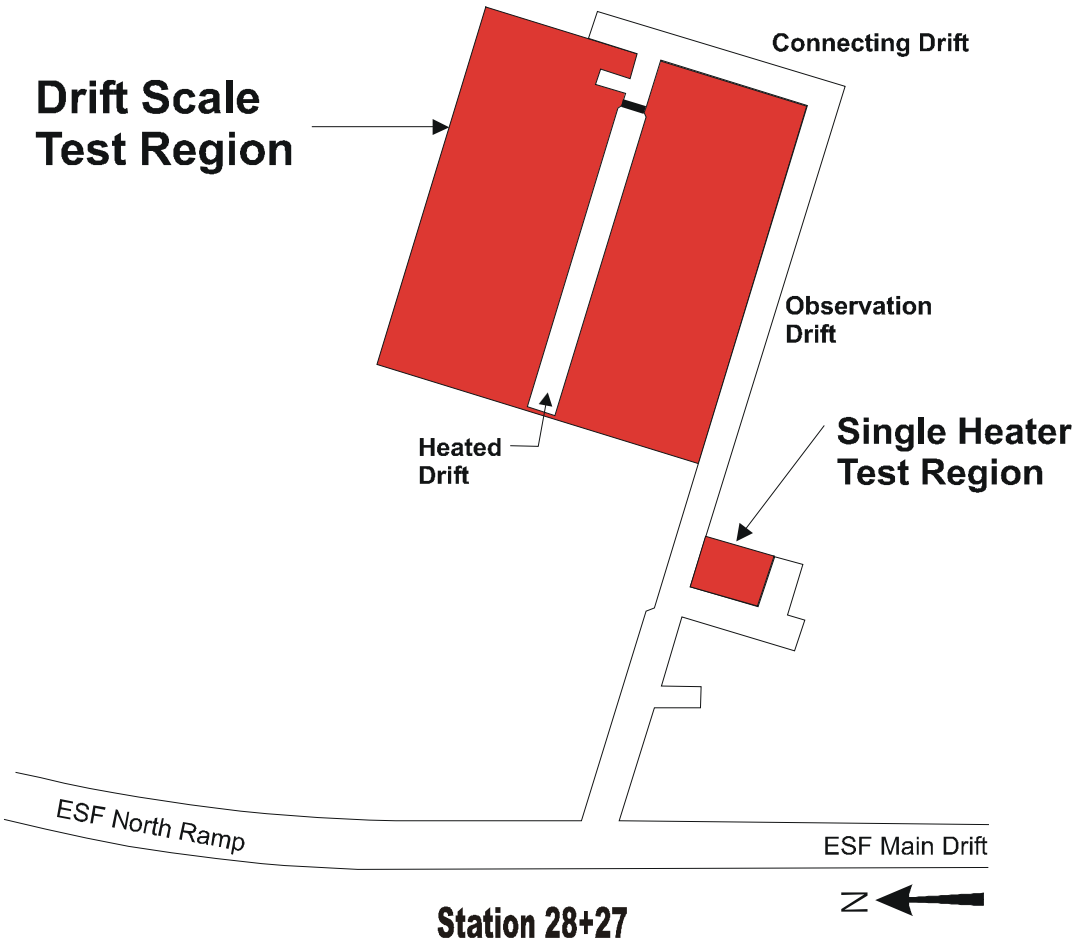

Figure 1. Schematic Plan View of ESF Thermal Test Facility Including the Single Heater test (SHT) and the Drift Scale Test (DST)

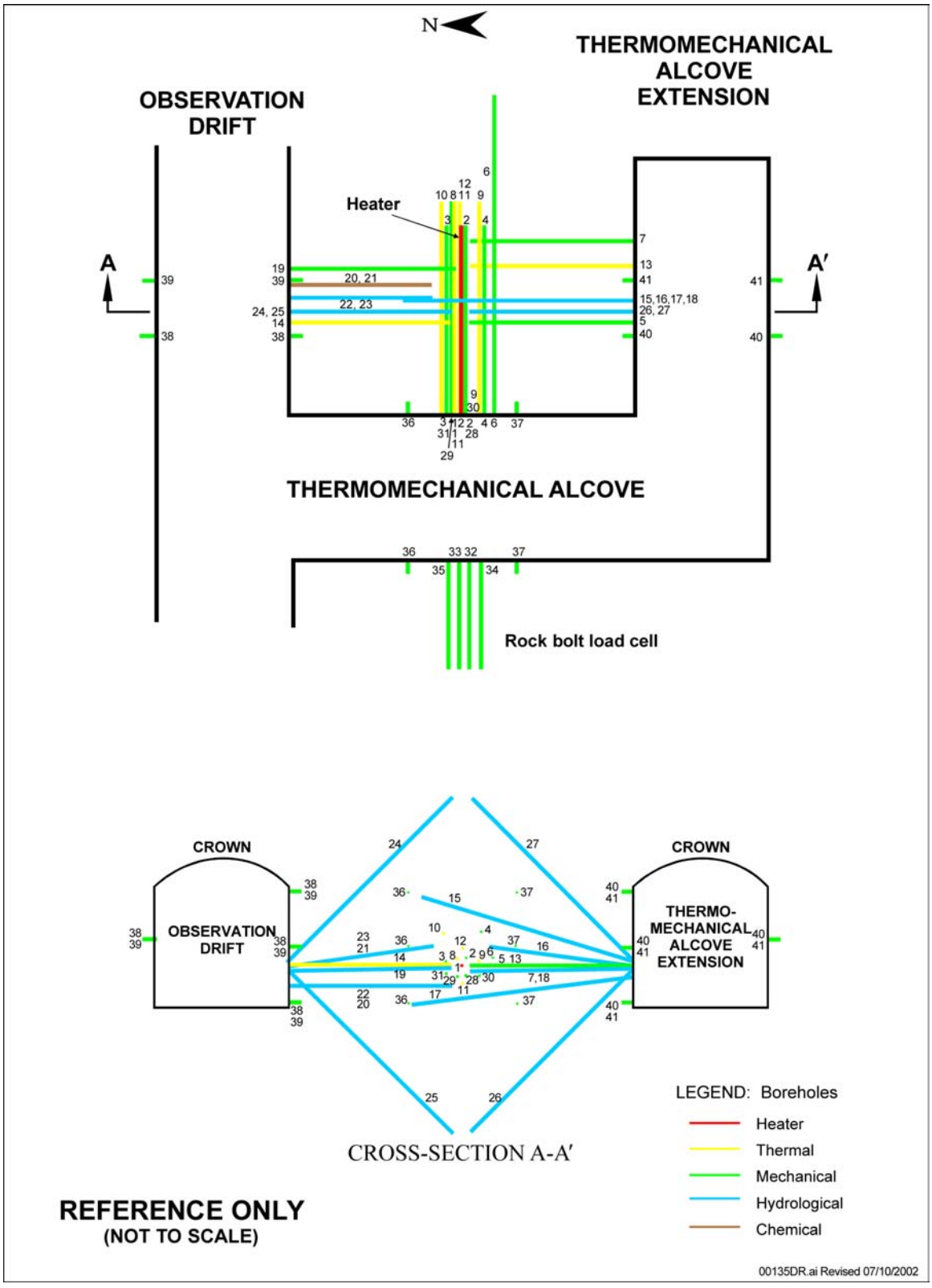

Figure 2. Schematic SHT Layout of the Instrumental Boreholes, Color Coded According to Their Functions

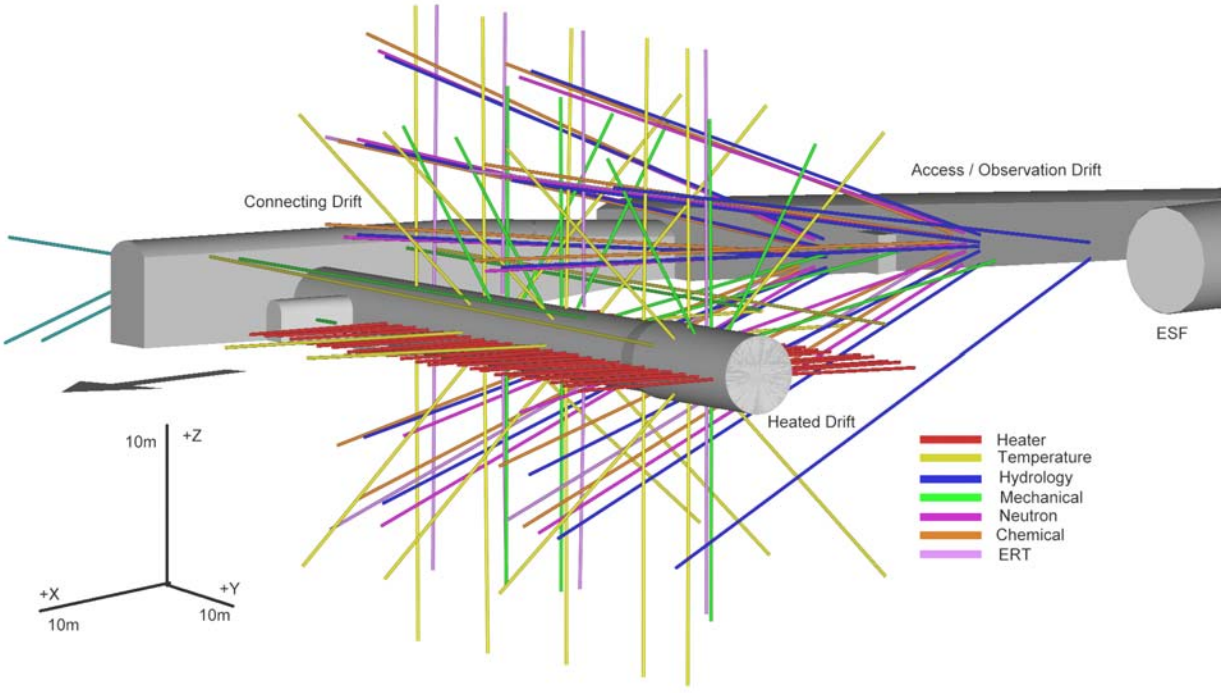
Access / Observation Drift
Connecting Drift
ESF
Heated Drift
Heater
Temperature
Hydrology
Mechanical
Neutron
Chemical
ERT
10m
+Z
+X
10m
+Y
10m

Figure 3. Perspective View Showing Drifts and Boreholes of the DST, Boreholes Are Color Coded According to Their Functions

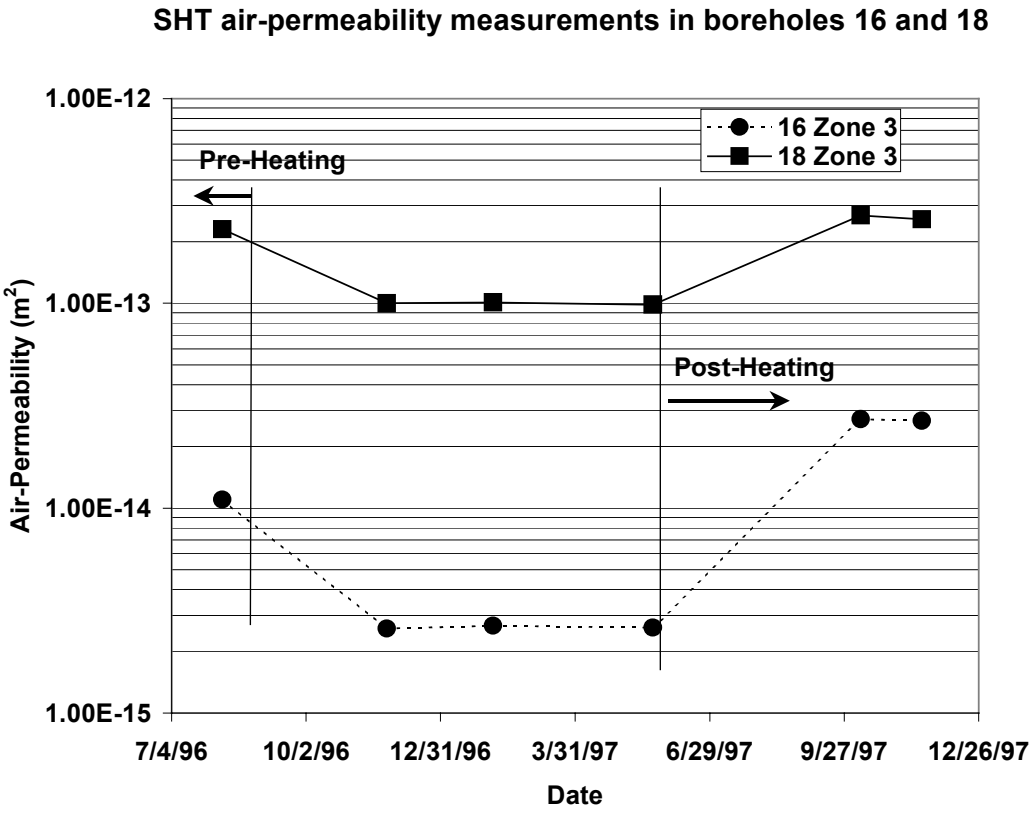

Figure 4. Air Permeability Measurements in Zone 3 of Boreholes 16 and 18 for before, during and after Heating phase of the SHT

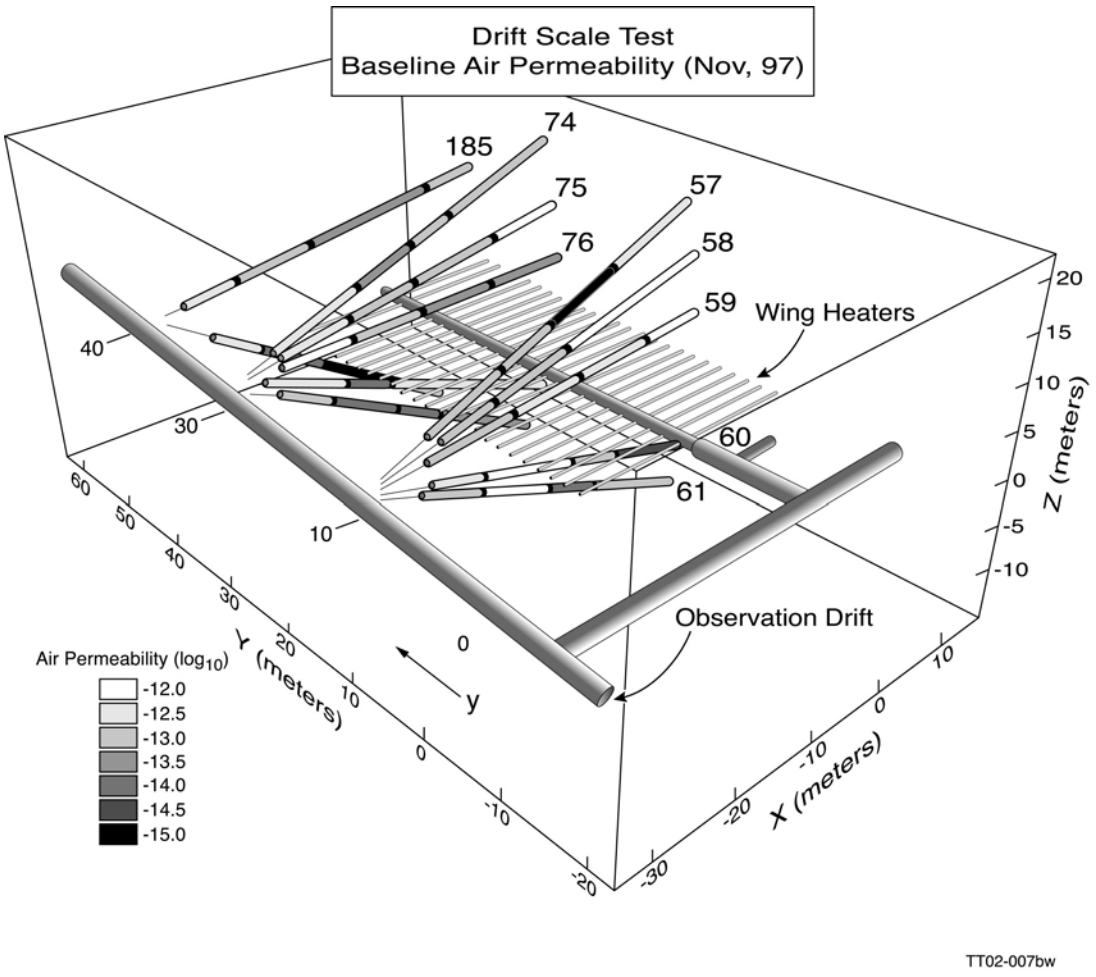

Figure 5. Preheating Baseline Permeability Measurements in Zones Isolated by Packers in Twelve 40 m Long Boreholes in the DST, the Permeability Values Range over Three Orders of Magnitude

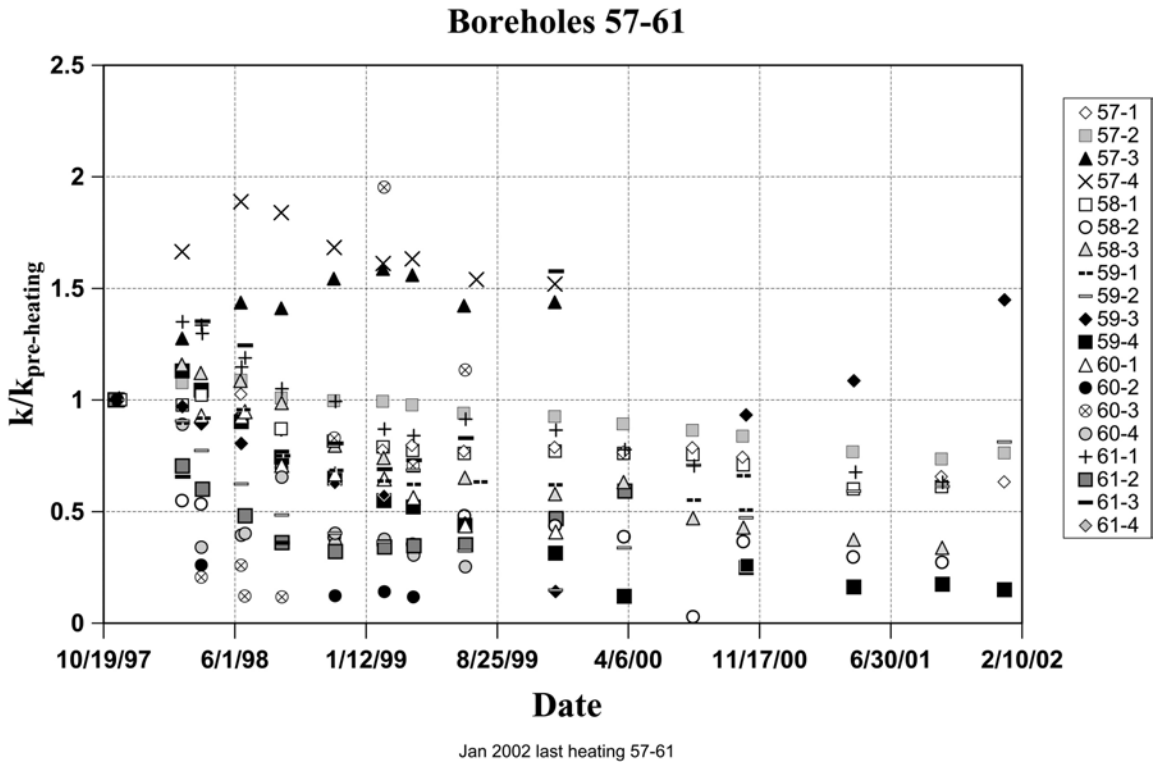

Figure 6. Changes in Permeability Displayed as Ratio to the Preheating Permeability Estimate for DST Boreholes 57-61

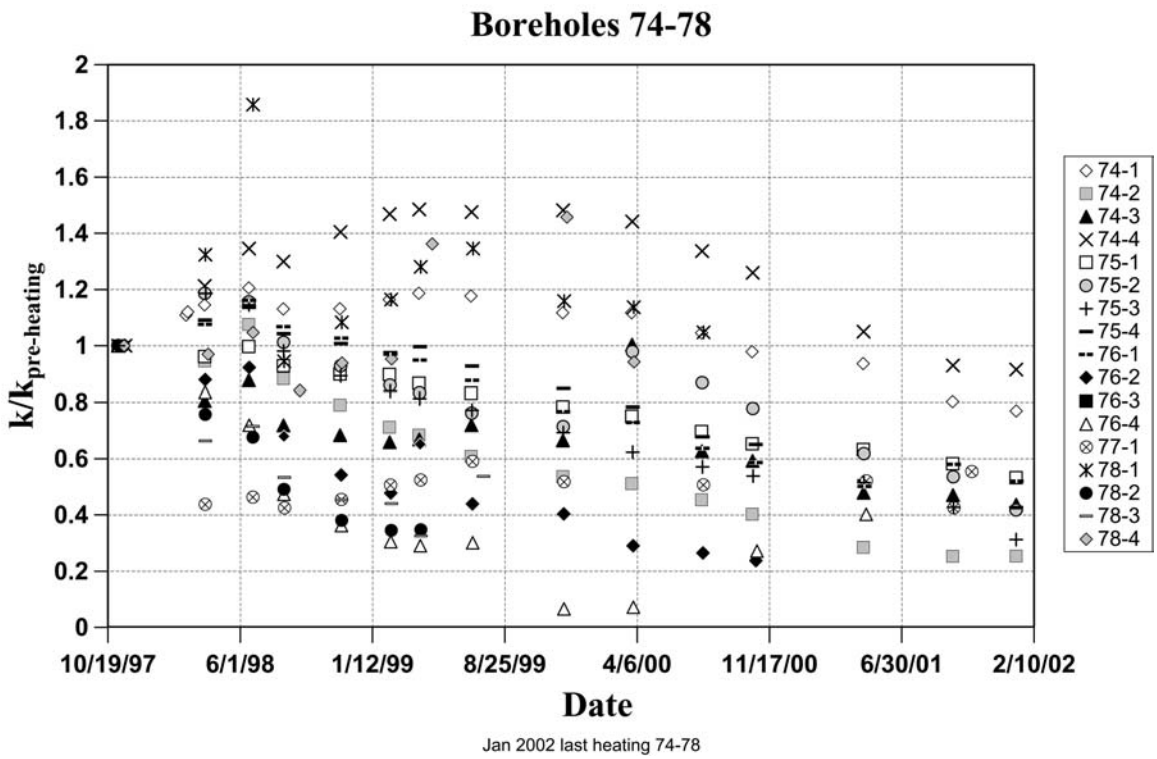

Figure 7. Changes in Permeability Displayed as Ratio to the Preheating Permeability Estimate for DST Boreholes 74-78

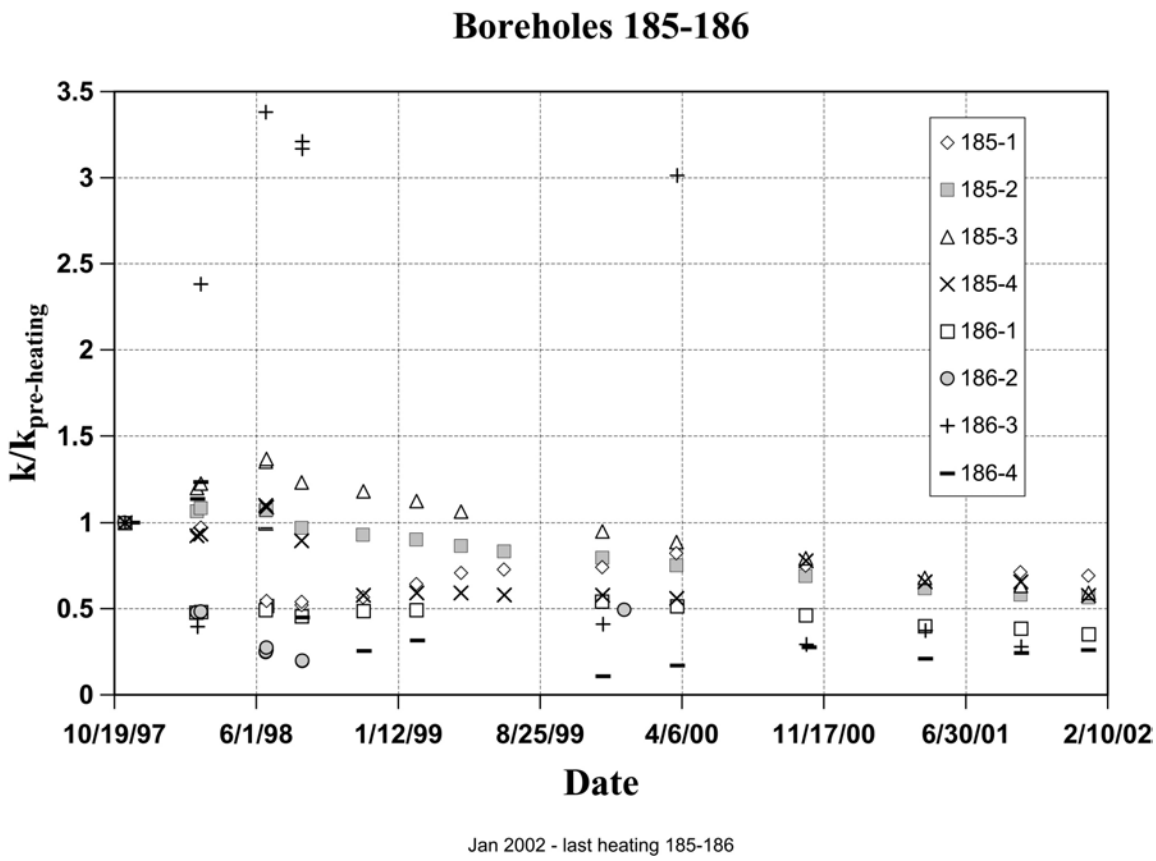

Figure 8. Changes in Permeability Displayed as Ratio to the Preheating Permeability Estimate for DST Boreholes 185-186